Analyst

ROYAL SOCIETY OF CHEMISTRY

PAPER

View Article Online
View Journal | View Issue

Cite this: *Analyst*, 2024, **149**, 3396

A quadratic isothermal amplification fluorescent biosensor without intermediate purification for ultrasensitive detection of circulating tumor DNA†

Zhaojie Wu,[a] Hongshan Zheng,[a] Yongjun Bian,[a] Jian Weng,[a] Ru Zeng[b] and Liping Sun *[a]

Circulating tumor DNA (ctDNA) is an auspicious tumor biomarker released into the bloodstream by tumor cells, offering abundant information concerning cancer genes. It plays a crucial role in the early diagnosis of cancer. However, due to extremely low levels in body fluids, achieving a simple, sensitive, and highly specific detection of ctDNA remains challenging. Here, we constructed a purification-free fluorescence biosensor based on quadratic amplification of ctDNA by combining nicking enzyme mediated amplification (NEMA) and catalytic hairpin assembly (CHA) reactions. After double isothermal amplification, this biosensor achieved an impressive signal amplification of nearly 10^7-fold, enabling it to detect ctDNA with ultra-sensitivity. And the detection limit of this biosensor is as low as 2 aM. In addition, we explored the influence of human serum on the performance of the biosensor and found that it showed favorable sensitivity in the presence of serum. This biosensor eliminates the need for an intermediate purification step, resulting in enhanced sensitivity and convenience. Thus, our purification-free fluorescent biosensor exhibits ultra-high sensitivity when compared to other biosensors and has the potential to serve as an effective diagnostic tool for early detection of cancer.

Received 26th March 2024,
Accepted 16th April 2024

DOI: 10.1039/d4an00460d

rsc.li/analyst

Introduction

According to the report of the International Agency for Research on Cancer, cancer has become one of the main causes of death of people all over the world.[1] Most cancer patients are currently diagnosed when the tumor has already formed or at an even later stage, missing the best treatment period. Therefore, early and accurate detection of cancer is crucial for timely treatment and improvement of the survival rate. Tissue biopsy is the gold standard for the diagnosis of malignant tumors, but there are risks of tumor metastasis, patient pain, bleeding, and infection. Compared with tissue biopsy, liquid biopsy is a noninvasive test that monitors various cancer-associated biomarkers in body fluids.[2] Circulating tumor DNA (ctDNA) is a kind of promising biomarker for liquid biopsy. It is produced by apoptotic/necrotic tumor cells and released into the blood circulation.[3] Detection of ctDNA is challenging due to its extremely low abundance in the circulatory system (<100 copies per mL) and its susceptibility to interference by high concentrations of wild-type cell-free DNA. Therefore, development of sensitive and selective ctDNA detection methods is emergent for clinical diagnosis.

Traditional ctDNA detection techniques include the quantitative polymerase chain reaction (qPCR), digital PCR, next-generation sequencing, *etc.*[4–8] Despite the high sensitivity of these methods, complicated data analysis and expensive equipment are their common drawbacks for ctDNA detection. Therefore, it is necessary to develop a convenient and ultra-sensitive ctDNA detection method. Biosensors are analytical devices that are sensitive to biomolecules and can convert concentrations into physical or chemical signals. They have attracted attention in biomedical applications due to many advantages such as high stability and strong specificity.[9] Meanwhile, the sensitivity of biosensors can be greatly improved by signal amplification strategies. Bai *et al.* achieved 10^{10}-fold amplification of the colorimetric signal by combination of the catalytic properties of zero-dimensional and two-dimensional nanomaterials.[10] Another strategy to amplify a biosensor's signal is DNA amplification technology, including the polymerase chain reaction and isothermal amplification. Isothermal amplification has gradually become an alternative

[a]*The Higher Educational Key Laboratory for Biomedical Engineering of Fujian Province, Research Center of Biomedical Engineering of Xiamen, Department of Biomaterials, College of Materials, Xiamen University, 422 Siming Nan Road, Xiamen 361005, China. E-mail: sunliping@xmu.edu.cn*
[b]*Department of Medical Oncology, The First Affiliated Hospital of Xiamen University, Xiamen, China*

† Electronic supplementary information (ESI) available. See DOI: https://doi.org/10.1039/d4an00460d

to PCR, and enables exponential amplification of nucleic acids at constant temperatures in a short time. Various isothermal amplification strategies have been developed, such as loop-mediated isothermal amplification (LAMP), rolling circle amplification (RCA), hybridization chain reaction (HCR), catalytic hairpin assembly (CHA), *etc*.[11–14] Although isothermal amplification can avoid the tedious thermal cycling process, it is still insufficient for a biosensor to detect trace amounts of ctDNA based on a single isothermal amplification cycle. Therefore, multiple cycles of isothermal amplification were used to amplify ctDNA.[15–17] Wang *et al*. constructed a quadratic amplification system using a DNAzyme-powered DNA walker and a HCR to detect miRNA.[18] However, magnetic separation and other separation methods are still used in cascading signal amplification processes.[19–21] It results in the depletion of intermediate products, subsequently affecting the detection efficiency.[22] For example, the recovery efficiency of DNA is only 46.7%–70.5% using the magnetic bead purification method.[23]

In this study, we constructed an ultrasensitive fluorescence biosensor based on quadratic isothermal amplification without any purification procedure. In the first amplification cycle, a large number of cDNAs were amplified by a nicking enzyme mediated amplification reaction, leading to 10^3-fold signal amplification. In the second cycle, the cDNA activated the CHA and further achieved 10^4-fold signal amplification. Thus, the sensitivity of this fluorescence biosensor is significantly enhanced and reaches 2 aM ctDNA. Our research provides a new method for simple and quick detection of ctDNA.

Materials and methods

Materials

Sodium chloride (NaCl), potassium chloride (KCl), potassium dihydrogen phosphate (KH_2PO_4), disodium hydrogen phosphate ($Na_2HPO_4{\cdot}12H_2O$), hydrogen tetrachloroaurate ($HAuCl_4$), and sodium citrate ($C_6H_5Na_3O_7$) were purchased from Sinopharm Chemical Reagent Co., Ltd (Beijing, China). Dithiothreitol (DTT) was purchased from Shanghai Acmec Biochemical Co., Ltd. Tris (2-carboxyethyl) phosphine hydrochloride (TCEP), NB.BbvCI, Klenow fragment, dNTP, 4S red plus, 50× TAE buffer, DNA Marker, and 30% acrylamide solution were purchased from Sangon Biotechnology Co., Ltd (Shanghai, China).

All oligonucleotides with different sequences were synthesized and HPLC purified by Sangon Biotechnology Co., Ltd (Shanghai, China). The sequences of the oligonucleotide are listed in Table S1.†

All experiments were performed in accordance with the Guidelines "Constitution of Medical Ethics Committee of Xiamen University School of Medicine", and approved by the ethics committee at Xiamen University. Informed consent was obtained from human participants of this study.

Synthesis of AuNPs

First, 250 μL of 50 mM $HAuCl_4$ was mixed with 50 mL of H_2O and heated until boiling with stirring. Subsequently, 3.5 mL of sodium citrate (1 wt%) was added quickly, heated and stirred for 10 minutes. The color of the solution changed from pale yellow to wine red in several minutes. Finally, the product was centrifuged at 12 000 rpm for 10 min, washed, and then redispersed in water to obtain AuNPs. The prepared AuNPs were stored at 4 °C.

Formation of hairpin DNA and conjugation of H1 with AuNPs

H1 and H2 DNA solutions were heated to 95 °C for 5 min and then cooled to room temperature at a cooling rate of 1 °C min^{-1} to form hairpin DNA structures. 1 μL of 50 mM TCEP was added to 100 μL of 5′ thiolated H1 (100 nM) and incubated at 37 °C for 1 hour to reduce disulfide bonds. Then the H1 solution was mixed with 200 μL of AuNP solution and stirred overnight at room temperature. After centrifugation at 12 000 rpm for 10 min and repeated washing, H1-modified AuNPs (H1-AuNPs) were obtained, resuspended in phosphate buffered saline (PBS) (10 mM, pH 7.4), and stored at 4 °C.

Detection of ctDNA

First, 10 μL of ctDNA and 10 μL of 100 nM template DNA were mixed and incubated at room temperature for 10 min. Then 2.5 μL of NEB 2.1 buffer (10×), 1 μL of 5 U L^{-1} Klenow fragment, 0.5 μL of 10 U L^{-1} NB.BbvCI, and 0.5 μL of 25 mM dNTP were added. Finally, ultrapure water was added to supplement the final volume to 50 μL. The reaction was carried out at 37 °C for 2 h to produce cDNA. Ultimately, the enzyme was inactivated by heating the solution at 85 °C for 20 min.

Afterward, the cDNA solution was mixed with 100 μL of 400 nM H2 and 100 μL of H1-AuNPs. The mixture was incubated at 37 °C for 2 h for CHA amplification. Then AuNPs were collected by centrifugation at 12 000 rpm for 10 min and washed with 10 mM PBS buffer (pH 7.4) 3 times, which can remove free H2 to significantly reduce background fluorescence. The precipitate was dispersed in 1 mL water and the fluorescence spectra were recorded at the excitation wavelength of 480 nm. The fluorescence emission intensity was measured at 518 nm.

Native polyacrylamide gel electrophoresis

15% polyacrylamide gel electrophoresis was performed in 1× TAE buffer solution (40 mM Tris-acetate, 1 mM EDTA, pH 8.0–8.6) at 110 V for 60 min. Then, the polyacrylamide gel was dyed with 4S Red Plus solution, and was further imaged under UV light using a ChemiDoc XRD system (Bio-Rad).

Results and discussion

Detection principle

The epidermal growth factor receptor (EGFR) gene plays a significant role in the diagnosis and management of non-small-cell lung cancer (NSCLC), which is responsible for approximately 85% to 90% of all lung malignancies.[1,24,25] In this study, we assessed ctDNA containing the EGFR exon 19 deletion mutation (Del 2235–2249, Table S1†).

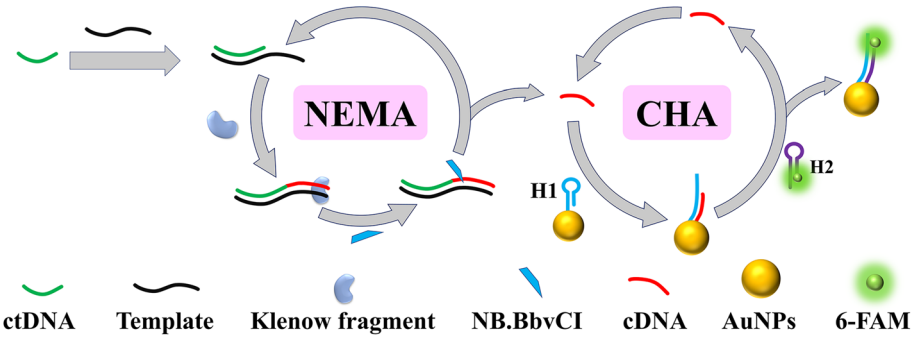

Fig. 1 The detection principle of the biosensor based on double signal amplification.

As shown in Fig. 1, in the first cycle of signal amplification, a ctDNA strand bound to the template DNA by complementary base pairing and was prolonged by *E. coli*. DNA polymerase I (Klenow fragment) to produce the recognition site of the nicking endonuclease NB.BbvCI. Next, the prolonged DNA strand was cut by the nicking enzyme to produce cDNA. The residual DNA fragment was prolonged by the Klenow fragment and cut by NB.BbvCI again. This process was continuously repeated to produce abundant cDNA to realize the primary signal amplification.

In the secondary signal amplification, the cDNA opened a H1 hairpin on the AuNP surface. The FAM-labeled H2 hairpin was opened by H1 DNA, and the cDNA was dissociated from H1. Then, the free cDNA opened another H1 hairpin and repeated the above process. As a result, more and more FAM-labeled H2 strands were attached to AuNPs, producing strong fluorescence. Therefore, as long as the free H2 was removed to reduce background fluorescence, the fluorescence intensity at 518 nm was then measured to achieve quantitative analysis.

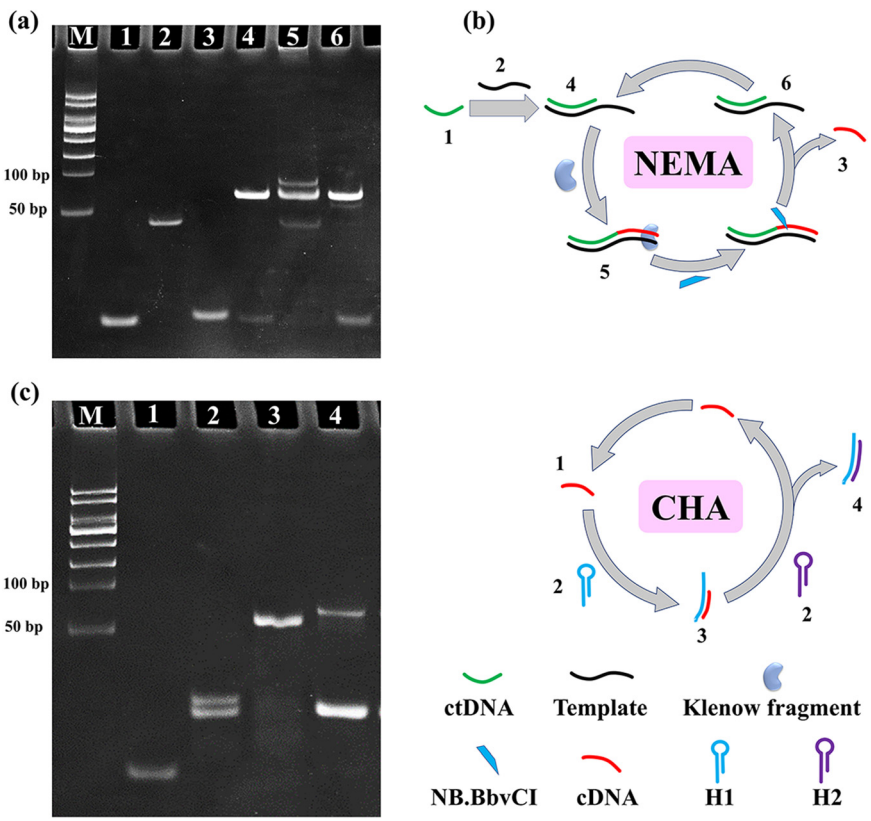

Fig. 2 Characterization of NEMA and CHA products. (a) Native PAGE of NEMA. M: Marker, lane 1: 2 μM ctDNA, lane 2: 2 μM template DNA, lane 3: 2 μM cDNA, lane 4: 1 μM ctDNA + 1 μM template DNA, lane 5: 1 μM ctDNA + 1 μM template DNA + 5 U Klenow fragment, lane 6: 1 μM ctDNA + 1 μM template DNA + 5 U Klenow fragment + 10 U NB.BbvCI. (b) Scheme of NEMA and scheme of CHA. The numbers indicate the corresponding lanes in (a) and (c). (c) Native PAGE of CHA. Lane 1: 1 μM cDNA, lane 2: 1 μM H1 + 1 μM H2, lane 3: 1 μM cDNA + 1 μM H1, lane 4: 0.25 μM cDNA + 1 μM H1 + 1 μM H2.

Between the primary and secondary amplification cycles, there was no purification step, which can not only simplify the experimental operation but also reduce the loss of ctDNA and enhance the sensitivity of the biosensor.

Characterization of DNA amplification by NEMA and CHA

Our biosensor depended on the signal amplification by isothermal amplification of DNA (NEMA and CHA). Native polyacrylamide gel electrophoresis was performed to verify these two processes. The results of NEMA are shown in Fig. 2a. Lane 1–3 represent the ctDNA, template DNA, and cDNA band, respectively (Fig. 2b). After the ctDNA hybridized with the complementary template DNA, a new product with larger molecular weight was formed (lane 4). Then the Klenow fragment bound to the DNA duplex and triggered the polymerization reaction, forming a higher band in lane 5. Afterward, the newly formed complex was cut by NB.BbvCI and cDNA was formed (the lower band in lane 6).

Fig. 2c shows the electrophoresis results of CHA. Lane 1 represents the cDNA band. The two bands close to each other in lane 2 are H1 (upper band, 61 bp) and H2 (lower band, 52 bp) hairpins, respectively. In the presence of cDNA, the H1 hairpin opened and hybridized with cDNA to form a cDNA/H1 complex, resulting in a new band in lane 3. Then H2 hybridized with H1 to form a H1/H2 complex (upper band in lane 4). The lower band was the product of unreacted excess H2. These results demonstrated that cDNA can be produced by nicking enzyme mediated amplification which triggered the hybridization of H1 and H2.

Performance of the biosensor

We optimized the reaction time and hairpin DNA concentration to achieve the best performance of the biosensor (Fig. S3†). 100 nM H1, 200 nM H2 and 2 h of reaction time were used for subsequent experiments. The fluorescence intensity gradually decreased with the decrease of ctDNA concentration. The limit of detection (LOD) reached as low as 2 aM (Fig. 3a) with a wide linear range of 100 aM–10 pM (correlation coefficient R^2 = 0.996, Fig. 3b). Compared with other fluorescent biosensors for nucleic acids using the isothermal amplification strategy or nanomaterials (Table S3†), this biosensor achieved a significantly lower detection limit (2×10^{-18} mol L^{-1}).

In order to evaluate the selectivity of this biosensor, we measured ctDNA, non-complementary (Random), one-base mismatch (Mismatch 1), two-base mismatch (Mismatch 2),

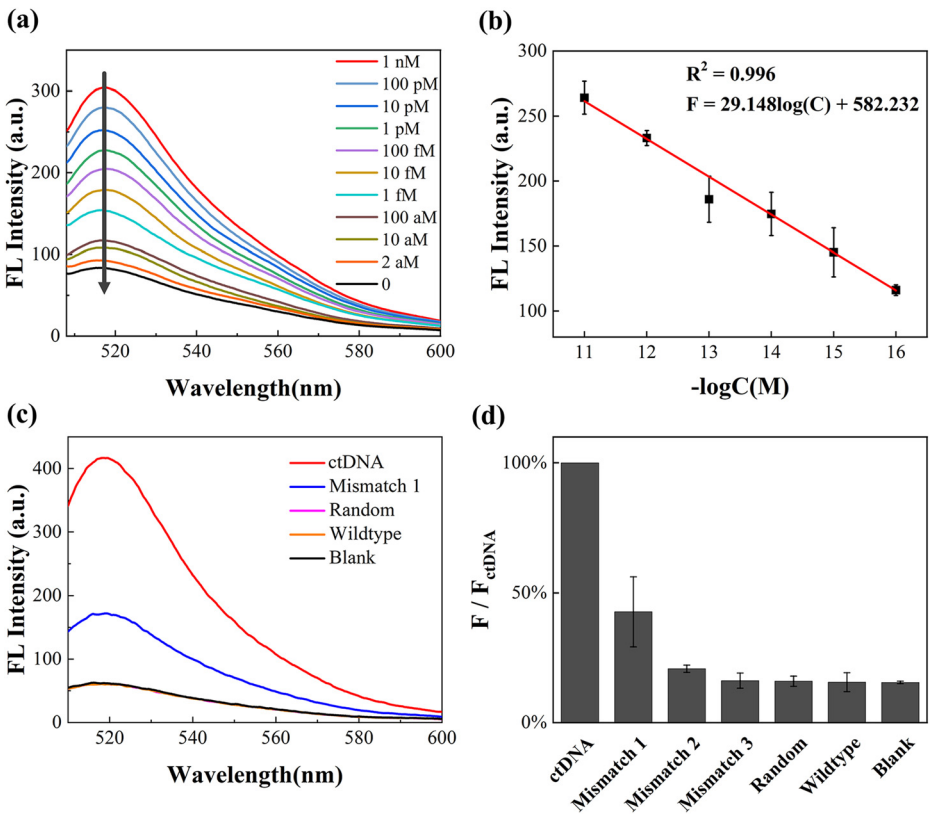

Fig. 3 The performance of the biosensor. (a) Fluorescence spectra of the present biosensor for different concentrations of ctDNA. (b) The linear relationship of the fluorescence intensity at 518 nm *versus* ctDNA concentration. (c) Fluorescence spectra of the biosensor for 10 nM ctDNA, Mismatch 1, Random, Wildtype, and Blank samples. Blank: Sample containing no ctDNA. (d) Selectivity test for the present biosensor for 10 nM non-complementary (Random), one-base mismatch (Mismatch 1), two-base mismatch (Mismatch 2), three-base mismatch (Mismatch 3), and unmutated (Wildtype) sequences. Control: Sample containing no ctDNA (n = 3). All experiments were conducted at 37 °C.

three-base mismatch (Mismatch 3), and unmutated (Wildtype) sequences, respectively (Table S1†). The sample containing ctDNA exhibited the highest fluorescence signal, while the fluorescence generated by Mismatch 1 and Mismatch 2 with two-base mismatch was reduced by 59% and 80%, respectively (Fig. 3c and d). The fluorescence signals of Mismatch 3, Random, and Wildtype sequences were nearly the same as that of the blank sample. M1 differs from ctDNA by only one base, thus Mismatch 1 can still bind to part of the template DNA, triggering subsequent amplification. However, compared with that of the completely complementary ctDNA, the amplification efficiency of Mismatch 1 was greatly weakened. These results demonstrated that our biosensor could differentiate one-base mutation of ctDNA.

The influence of intermediate products on the performance of the biosensor

The intermediate products between the NEMA and HCA amplification cycles include cDNA, ctDNA, template DNA, Klenow fragment, NB.BbvCI, and non-specific amplification products from NEMA, which might disturb CHA amplification (Table S2†). Therefore, we explored the effects of these products on downstream reactions. As shown in Fig. 4a, cDNA, template DNA, and their mixtures have little effect on the subsequent reaction.

In order to reduce the influence of enzymes on the subsequent CHA reaction, we heated the samples to inactivate the Klenow fragment and NB.BbvCI. As we know, the Klenow fragment resembles a half-open right hand and consists of four subdomains: the 3′-to-5′ exonuclease, the thumb, the palm, and the fingers subdomain. The DNA template–primer duplex is bound in a shallow cleft between the thumb and 3′ *exo* domains, and the new strand is synthesized in the fingers subdomain[26] (Fig. S6a†). Nb.BbvCI is composed of two non-identical subunits and resembles a windmill[27] (Fig. S6b†). It can recognize CCTNAGC (N = any base) and cut only the bottom strand of the target site[27] (Fig. S6c†). Heating will cause irreversible damage to the structures of the Klenow fragment and Nb.BbvCI, resulting in enzyme inactivation and disruption of DNA replication and sequence recognition.[28,29]

We investigated the impacts of both the inactive enzyme and the active enzyme on the subsequent reaction. The final

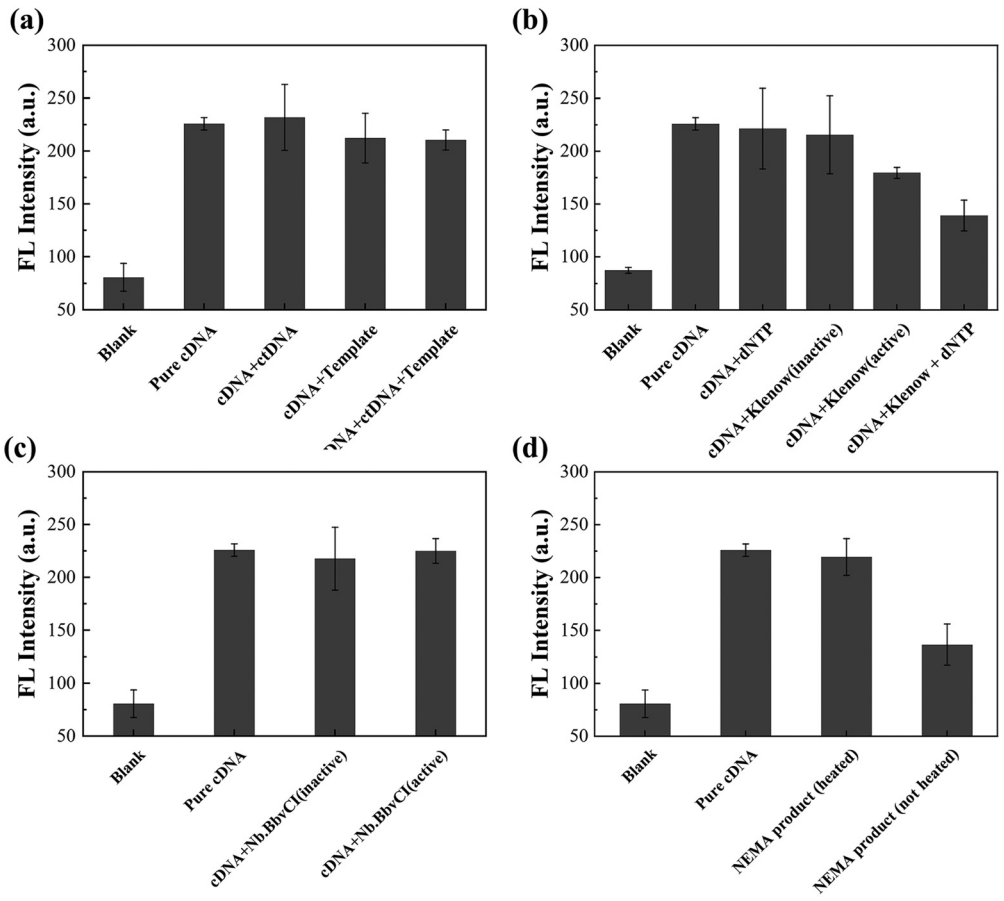

Fig. 4 Influence of NEMA products on the fluorescence intensity of the biosensor (n = 3). (a) The influence of DNA on the fluorescence intensity (0.1 nM cDNA, 1 nM target, 100 nM template DNA). (b) The influence of the Klenow fragment on the fluorescence intensity. The Klenow fragment was inactivated by heating at 95 °C for 20 min (0.1 nM cDNA, 1 mM dNTP, 5 U Klenow fragment). (c) The influence of NB.BbvCI on the fluorescence intensity. NB.BbvCI was inactivated by heating at 95 °C for 20 min (0.1 nM cDNA, 10 U NB.BbvCI). (d) Effect of NEMA products on the fluorescence intensity before and after heating at 95 °C for 20 min.

fluorescence intensity of the biosensor was reduced if the Klenow fragment was not deactivated by heating (Fig. 4b). But the effect can be eliminated by deactivation of the Klenow fragment. As previously reported, in the presence of dNTP, the Klenow fragment demonstrated the ability to elongate the second strand of hairpin DNA by utilizing the sticky ends as a template.[30] As a result, blunt-end stem–loop DNA was generated, which lacks functionality and prevents secondary amplification.

Meanwhile, as shown in Fig. 4c, the fluorescence intensity remained largely unaltered regardless of the state of NB.BbvCI. Thus, NB.BbvCI did not affect the secondary signal amplifica-

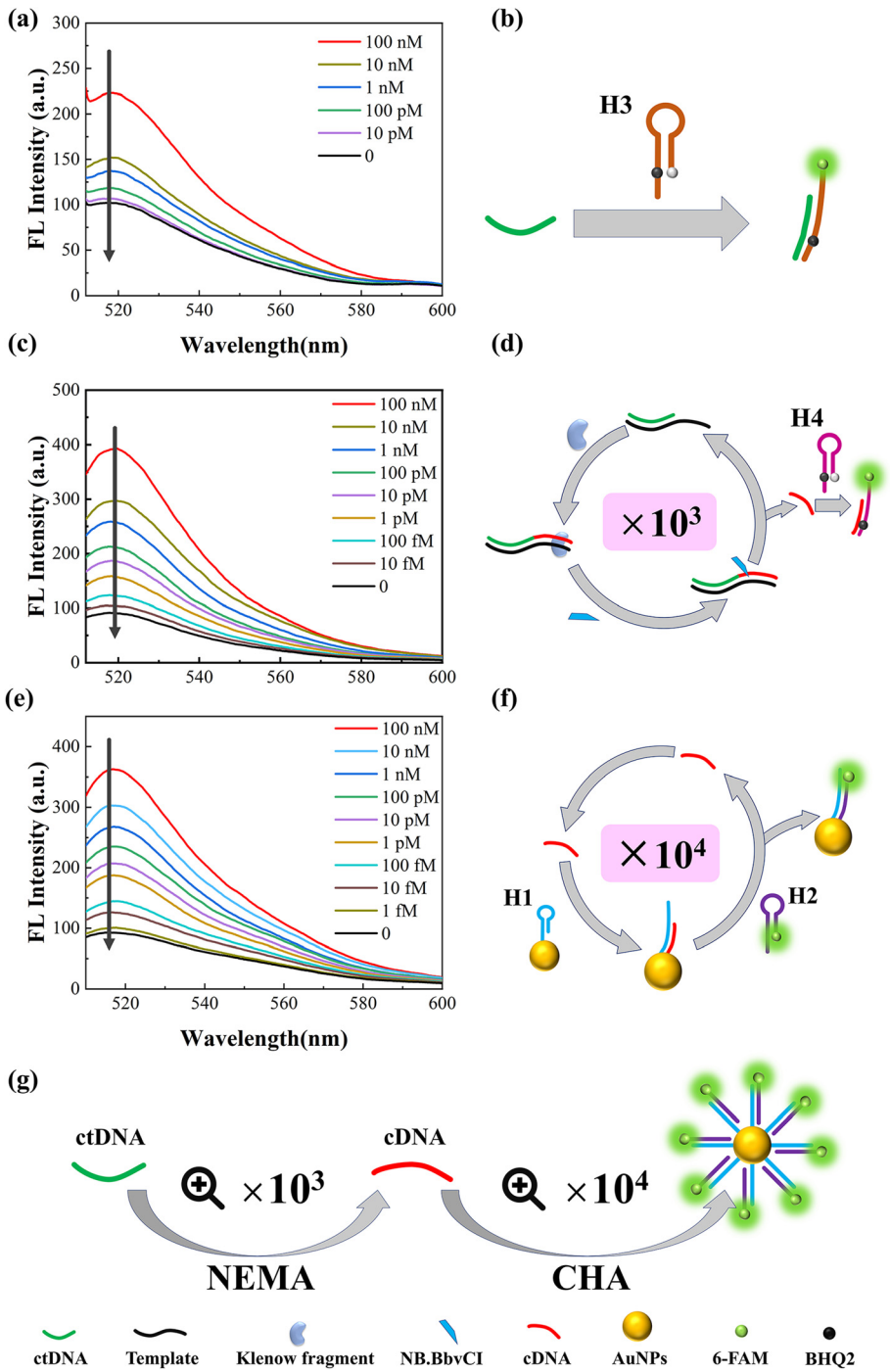

Fig. 5 Mechanism of the signal amplification. (a) Fluorescence spectra of the biosensor without any signal amplification for different concentrations of ctDNA. (b) The detection principle of the biosensor without any signal amplification. (c) Fluorescence spectra of the biosensor with signal amplification by enzyme reactions for different concentrations of ctDNA. (d) The detection principle of the biosensor with signal amplification by enzyme reactions. (e) Fluorescence spectra of the biosensor with signal amplification by CHA reactions for different concentrations of ctDNA. (f) The detection principle of the biosensor with signal amplification by CHA reactions. (g) Double signal amplification of the fluorescence biosensor.

tion. We also compared the effects of heated and unheated NEMA products and found that the heated product did not influence the fluorescence intensity of the biosensor, while the unheated NEMA product-participating HCA showed significantly reduced fluorescence intensity compared with the effects of pure cDNA (Fig. 4d).

In conclusion, all products of the primary signal amplification (NEMA) had little impact on the secondary signal amplification (CHA) under heating conditions, indicating that the intermediate purification step was unnecessary for our biosensor. This purification-free fluorescent biosensor based on quadratic isothermal amplification could provide a fast and convenient tool for ctDNA detection.

Signal amplification mechanism

Our fluorescence biosensor is based on a two-step signal amplification strategy. First, the NEMA reaction produced a large amount of cDNA. Then the CHA reaction further amplified the signal of the biosensor by generating a lot of H1/H2 duplexes. To explore the signal amplification efficiency of each step, we separately studied these two steps and compared the results with that of the fluorescent biosensor without signal amplification (Fig. 5a). H3 hairpin DNA complementary to ctDNA was designed to detect ctDNA. The detection limit of this biosensor without any signal amplification is only 10^{-11} M (10 pM, Fig. 5b).

Next, H4 hairpin DNA complementary to cDNA was designed to investigate the signal amplification of the NEMA reaction (Fig. 5d). As shown in Fig. 5c, NEMA improved the detection limit of the biosensor to 10^{-14} M (10 fM), which was 10^3 times that of the biosensor without isothermal amplification (Fig. 5a and b). The CHA reaction further reduced the detection limit to 10^{-14} M (1 fM, Fig. 5e and f), resulting in 10^4-fold signal amplification, similar to previous reports by Li *et al.*[31] The combination of NEMA and CHA reactions achieved nearly 10^7-fold signal amplification, which is consistent with our results in Fig. 3 (LOD 2 aM). We also calculated the amplification efficiency of NEMA and CHA according to the activity of the enzymes and the rate of CHA (ESI 2.4†). We found that the signal could be amplified 5.2×10^3 fold by NEMA and 9.6×10^3 fold by CHA, respectively. This result is close to our experimental results (10^3-fold for NEMA and 10^4-fold for CHA amplification).

Effect of serum on the performance of the biosensor

Given that the majority of proteins present in human serum are predominantly albumin (Table S4†), we employed bovine serum albumin (BSA) to further investigate the impact of serum on our biosensor.[32] As depicted in Fig. 6a, the fluo-

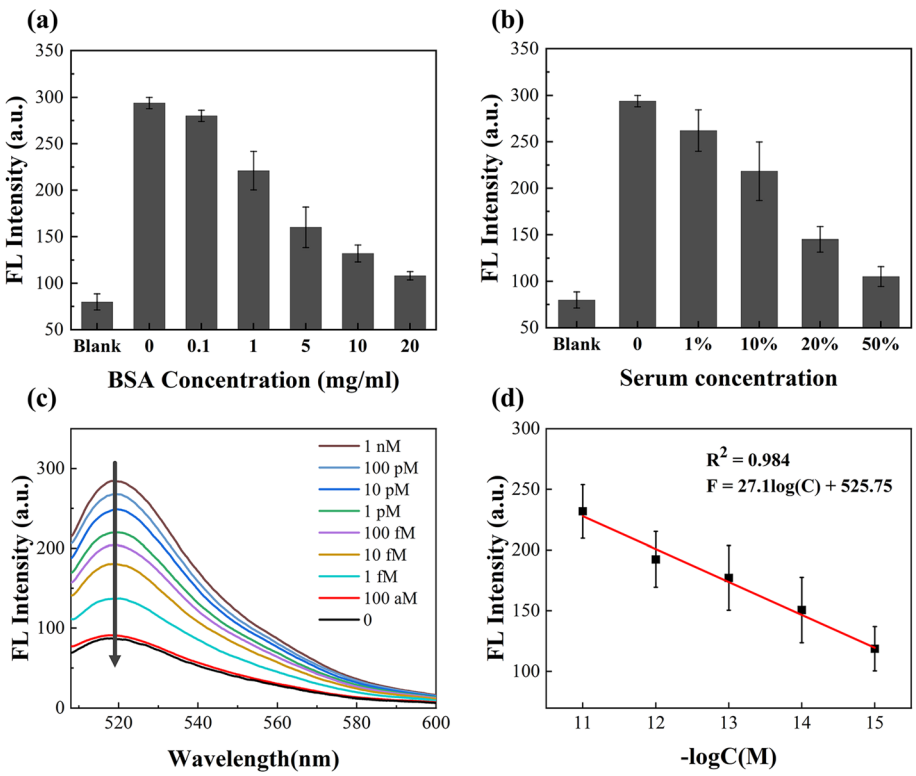

Fig. 6 The performance of the biosensor in PBS containing human serum. (a) Fluorescence intensity of the present biosensor for ctDNA in PBS containing different concentrations of BSA (n = 3). (b) Fluorescence intensity of the present biosensor for ctDNA in PBS containing different contents of human serum (n = 3). (c) Fluorescence spectra of the present biosensor for different concentrations of ctDNA in PBS containing 1% (v/v) human serum. (d) The linear relationship of the fluorescence intensity at 518 nm *versus* the negative logarithm of ctDNA concentration (n = 3). All experiments were conducted at 37 °C.

Table 1 Determination of the recovery rate in the detection of ctDNA

Serial number	ctDNA sample concentration (pM)	Detection concentration (pM)	RSD (n = 3)	Recovery (%)
1	10	9.96 ± 1.03	0.103	99.6
2	1	1.02 ± 0.19	0.186	102
3	0.1	0.0931 ± 0.0083	0.089	93.1

All experiments were conducted in 1% human serum.

rescence intensity decreased with the increase of BSA concentration. BSA can be adsorbed onto AuNPs by electrostatic attraction and covalent binding *via* cysteine residues, resulting in a BSA corona around the AuNP surface.[33,34] At low BSA concentrations (<0.1 mg ml^{-1}), a tiny amount of adsorbed BSA resulted in a minor BSA corona on the surface of AuNPs, which has no impact on DNA hybridization. But at high BSA concentrations, a large BSA corona is formed on the AuNP surface, inhibiting the hybridization of DNA and thereby compromising the CHA process.[35]

To monitor clinical serum samples, we added ctDNA in PBS containing different contents of human serum. As shown in Fig. 6b, the fluorescence intensity exhibited a gradual decline as the concentration of human serum increased. But at 1% human serum, there was little influence on the fluorescence. Consequently, we used PBS containing 1% human serum to further study the performance of our biosensor. As shown in Fig. 6c, the detection limit reached 100 aM. There was still a good linear relationship between the negative logarithm of ctDNA concentration and the corresponding fluorescence intensity in the range of 1 fM to 10 pM (R^2 = 0.996). These results confirmed that our biosensor has high sensitivity and selectivity in serum. Compared with the detection in serum-free PBS (Fig. 3a), the sensitivity of this biosensor decreased 10 times. This phenomenon might be attributed to the unavoidable interference caused by the non-specific adsorption of proteins present in serum samples, which adversely affects the performance of the biosensor.[36]

We conducted a sample addition recovery experiment to assess the accuracy of our biosensor. Under optimal experimental conditions, we detected three different concentrations of ctDNA (0.1, 1, and 10 pM) in PBS containing 1% human serum. As shown in Table 1, the recovery rate of ctDNA ranged from 93.1% to 102%, with the relative standard deviation (RSD) ranging between 8.9% and 18.6%. These results demonstrated the high accuracy of our biosensor.

Conclusions

In our work, based on double signal amplification, a purification-free fluorescent biosensor was constructed to detect ctDNA. The signal of the biosensor is amplified by quadratic NEMA and CHA isothermal amplification and it achieves ultrasensitive detection of ctDNA (2 aM). Besides, our biosensor can discriminate single-nucleotide mutation with high selectivity. Our study provided theoretical and technical foundations for practical applications of this biosensor. In the future, we will collect blood samples from lung cancer patients carrying the EGFR exon 19del mutation to assess the practical applicability and diagnostic accuracy of this biosensor.

Author contributions

Zhaojie Wu: data curation and writing – original draft. Hongshan Zheng: visualization and validation. Yongjun Bian: project administration. Jian Weng and Ru Zeng: conceptualization and methodology. Liping Sun: conceptualization, methodology, funding acquisition, supervision, and writing – review & editing.

Conflicts of interest

There are no conflicts to declare.

Acknowledgements

This work was supported by the National Natural Science Foundation of China [81872415].

References

1 H. Sung, J. Ferlay, R. L. Siegel, M. Laversanne, I. Soerjomataram, A. Jemal and F. Bray, *CA-Cancer J. Clin.*, 2021, **71**, 209–249.
2 K. Pantel and C. Alix-Panabieres, *Nat. Rev. Clin. Oncol.*, 2019, **16**, 409–424.
3 L. Gorgannezhad, M. Umer, M. N. Islam, N.-T. Nguyen and M. J. A. Shiddiky, *Lab Chip*, 2018, **18**, 1174–1196.
4 P.-S. Kok, K. Lee, S. Lord, J. C.-H. Yang, R. Rosell, K. Goto, T. John, Y.-L. Wu, T. S. K. Mok and C. K. Lee, *Lung Cancer*, 2021, **154**, 113–117.
5 S. Mondaca, E. S. Lebow, A. Namakydoust, P. Razavi, J. S. Reis-Filho, R. Shen, M. Offin, H.-Y. Tu, Y. Murciano-Goroff, C. Xu, A. Makhnin, A. Martinez, N. Pavlakis, S. Clarke, M. Itchins, A. Lee, A. Rimner, D. Gomez, G. Rocco, J. E. Chaft, G. J. Riely, C. M. Rudin, D. R. Jones, M. Li, T. Shaffer, S. A. Hosseini, C. Bertucci, L. P. Lim, A. Drilon, M. F. Berger, R. Benayed, M. E. Arcila, J. M. Isbell and B. T. Li, *Lung Cancer*, 2021, **159**, 66–73.
6 P. Pisapia, U. Malapelle and G. Troncone, *Acta Cytol.*, 2019, **63**, 489–496.
7 E. Visser, R. de Kock, S. Genet, B. V. D. Borne, M. Y.-E. Soud, H. Belderbos, G. Stege, M. de Saegher, S. V. T. Westeinde, M. Broeren, F. Eduati, B. Deiman and V. Scharnhorst, *Transl. Oncol.*, 2023, **27**, 101589.
8 J. Zheng, Y. Wang, C. Hu, M. Zhu, J. Li, C. Lin, C. Lu, Y. Dou, C. Zhao, Y. Zhang, D. Wu, L. Li, H. Tang, T. He,

C. Pan, R. Han and Y. He, *Transl. Oncol.*, 2022, **13**, 3162–3173.
9 X. Yu, S. Zhang, W. Guo, B. Li, Y. Yang, B. Xie, K. Li and L. Zhang, *Sensors*, 2021, **21**, 7109.
10 Y. Bai, H. Li, J. Xu, Y. Huang, X. Zhang, J. Weng, Z. Li and L. Sun, *Biosens. Bioelectron.*, 2020, **166**, 112424.
11 Z. Duan, Z. Li, J. Dai, H. He and D. Xiao, *Talanta*, 2017, **164**, 34–38.
12 X. H. Li, X. L. Zhang, J. Wu, N. Lin, W. M. Sun, M. Chen, Q. S. Ou and Z. Y. Lin, *Talanta*, 2019, **191**, 277–282.
13 Z. W. Wong and S. Y. New, *Microchim. Acta*, 2022, **190**, 16.
14 Y. X. Zhao, F. Chen, Q. Li, L. H. Wang and C. H. Fan, *Chem. Rev.*, 2015, **115**, 12491–12545.
15 M. Hu, J. Wang, J. Han, Y. Rong, H. Yu, S. Ge, H. Yang, L. Zhang and J. Yu, *Sens. Actuators, B*, 2022, **369**, 132374.
16 M. Liang, M. Pan, J. Hu, F. Wang and X. Liu, *ChemElectroChem*, 2018, **5**, 1380–1386.
17 H. Ma, B. Guo, X. Yan, T. Wang, H. Que, X. Gan, P. Liu and Y. Yan, *RSC Adv.*, 2019, **9**, 19347–19353.
18 R. Wang, L. Wang, X. W. Xu and W. Jiang, *Sens. Actuators, B*, 2018, **268**, 287–292.
19 R. Wang, L. Wang, X. Xu and W. Jiang, *Sens. Actuators, B*, 2018, **268**, 287–292.
20 W. Wang, Y. Peng, J. Wu, M. Zhang, Q. Li, Z. Zhao, M. Liu, J. Wang, G. Cao, J. Bai and Z. Gao, *Anal. Chem.*, 2021, **93**, 4488–4496.
21 Y. Wang, X. Zhao, M. Zhang, X. Sun, J. Bai, Y. Peng, S. Li, D. Han, S. Ren, J. Wang, T. Han, Y. Gao, B. Ning and Z. Gao, *Anal. Chim. Acta*, 2020, **1116**, 1–8.
22 H. Jiang, Y. Li, X. F. Lv, Y. L. Deng and X. Q. Li, *Talanta*, 2023, **260**, 124645.
23 P. P. Li, M. H. Li, D. M. Yue and H. X. Chen, *J. Sep. Sci.*, 2022, **45**, 172–184.
24 R. Califano, O. Romanidou, G. Mountzios, L. Landi, F. Cappuzzo and F. Blackhall, *Drugs*, 2016, **76**, 831–840.
25 M. D. Siegelin and A. C. Borczuk, *Lab. Invest.*, 2014, **94**, 129–137.
26 J. Hohlbein and A. N. Kapanidis, in *Methods in Enzymology*, ed. M. Spies and Y. R. Chemla, Academic Press, 2016, ch. 581, 353–378.
27 B. W. Shen, L. Doyle, P. Bradley, D. F. Heiter, K. D. Lunnen, G. G. Wilson and B. L. Stoddard, *Nucleic Acids Res.*, 2019, **47**, 450–467.
28 D. F. Heiter, K. D. Lunnen and G. G. Wilson, *J. Mol. Biol.*, 2005, **348**, 631–640.
29 K. Bebenek, C. M. Joyce, M. P. Fitzgerald and T. A. Kunkel, *J. Biol. Chem.*, 1990, **265**, 13878–13887.
30 Y. Nishikawa and T. Sugiyama, *J. Gene Med.*, 2010, **12**, 927–933.
31 B. Li, Y. Liu, Y. Liu, T. Tian, B. Yang, X. Huang, J. Liu and B. Liu, *ACS Nano*, 2020, **14**, 8116–8125.
32 B. K. Sah and S. Kundu, *AIP Conf. Proc.*, 2020, **2265**, 030266.
33 D.-H. Tsai, F. W. DelRio, A. M. Keene, K. M. Tyner, R. I. MacCuspie, T. J. Cho, M. R. Zachariah and V. A. Hackley, *Langmuir*, 2011, **27**, 2464–2477.
34 E. Casals, T. Pfaller, A. Duschl, G. J. Oostingh and V. Puntes, *ACS Nano*, 2010, **4**, 3623–3632.
35 R. Wu, H. P. Peng, J. J. Zhu, L. P. Jiang and J. W. Liu, *Front. Chem.*, 2020, **8**, 121.
36 V. Singh, A. Nand, Sarita, J. Zhang and J. Zhu, *Arabian J. Chem.*, 2019, **12**, 3038–3045.